J Mater Sci (2007) 42:7657–7666
DOI 10.1007/s10853-007-1662-2

Cracking in the stir zones of Mg-alloy friction stir spot welds

Motomichi Yamamoto · Adrian Gerlich · Thomas H. North · Kenji Shinozaki

Received: 5 December 2006 / Accepted: 5 March 2007 / Published online: 3 June 2007

Abstract Liquid penetration induced (LPI) cracking is investigated during friction stir spot weld of AZ91, AZ31 and AM60 magnesium alloys. A combination of stir zone temperature measurement and detailed metallography has revealed differences in the cracking tendencies of different magnesium alloys when the dwell time during spot welding is varied. LPI cracking in AZ91 spot welds involves the following sequence of events: the formation of $\alpha - Mg + Mg_{17}Al_{12}$ eutectic films in the thermo-mechanically affected zone (TMAZ) region immediately adjacent to the stir zone extremity, engulfment of melted eutectic films as the stir zone width increases during the dwell period, penetration of α–Mg grain boundaries and crack propagation when torque is applied by the rotating tool. Cracking occurs early in the dwell period during AZ91 spot welding and almost the entire stir zone is removed when the rotating tool is withdrawn. However, crack-free AZ31 and AM60 spot welds are produced when a dwell time of 4 s is used since the stir zone temperatures are much higher than the α-Mg + $Mg_{17}Al_{12}$ eutectic temperature (437 °C) and melted eutectic films dissolve rapidly following their engulfment by the growing stir zone. In contrast, the temperature during the dwell period in AZ91 spot welding is close to 437 °C and melted eutectic films are not completely dissolved so that spot welds produced using a dwell time of 4 s exhibit LPI cracking.

M. Yamamoto (✉) · K. Shinozaki
Department of Mechanical System Engineering,
Graduate School of Engineering, Hiroshima University, 1-4-1,
Kagamiyama, Higashi-Hiroshima, Hiroshima 739-8527, Japan
e-mail: motoyama@hiroshima-u.ac.jp

K. Shinozaki
e-mail: kshino@hiroshima-u.ac.jp

A. Gerlich · T. H. North
Department of Materials Science and Engineering,
University of Toronto, 184 College St., Rm.140, Toronto,
Canada M5S3E4

A. Gerlich
e-mail: gerlich@ecf.utoronto.ca

T. H. North
e-mail: north@ecf.utoronto.ca

Introduction

Recently there is much interest in friction stir spot welding of magnesium alloys for automotive applications since these alloys can provide significant reductions in weight [1–4]. Although it is generally assumed that friction stir seam and friction stir spot welds are free of many of the defect formation issues that are commonly associated with fusion welding, liquid penetration induced (LPI) cracking has been recently found in the stir zones of AZ91 friction stir spot welds [5–8]. It has been suggested that the factors, which determine cracking during AZ91 friction stir spot welding comprise:

(i) Stir zone and thermo-mechanically affected zone (TMAZ) temperatures ≥437 °C during the dwell period in spot welding
(ii) Formation of melted eutectic films early in the dwell period, which are engulfed as the stir zone grows in width during the dwell periods in spot welding
(iii) Penetration of equiaxed α–Mg grain boundary regions by melted eutectic in the stir zone close to its extremity
(iv) Crack propagation when torque is applied as the tool rotates during the dwell period in spot welding

The nomenclature used to describe the mode of failure observed in the stir zone of AZ91 spot welds—liquid penetration induced cracking—emphasizes the important role played by melted eutectic in facilitating failure [5]. However, the peak temperatures attained in the stir zones of AZ31 and AM60 friction stir spot welds also exceed the $(\alpha - Mg + Mg_{17}Al_{12})$ eutectic temperature (437 °C in the Mg–Al binary equilibrium phase diagram) [9]. It is worth noting that the experimentally-measured eutectic temperatures found during casting of AZ91 and AM60 are 433 °C and 437 °C [10, 11]. With this in mind, the LPI cracking tendencies during AZ91, AZ31 and AM60 spot welding are investigated and compared in the present paper. It is shown that cracking occurs early in the dwell period in AZ91 spot welding and that almost the entire stir zone is removed when the rotating tool is withdrawn. In contrast, although cracking only occurs very early in the dwell period during AZ31 and AM60 spot welding crack-free joints are produced when a dwell time of 4 s is applied.

Experimental procedure

All friction stir spot welding trials were carried out using the following test sections:

(a) 3–8 mm thick × 25 mm diameter sections of a thixomolded semi-solid AZ91 extrusion having the chemical composition Mg 9wt.%Al 0.7wt.%Zn.
(b) 2.6 mm × 25 mm × 25 mm sections of a wrought AZ31 sheet having the chemical composition Mg 3wt.%Al 1wt.%Zn.
(c) 2.6 mm × 25 mm × 25 mm sections of a thixomolded AM60 sheet having the chemical composition Mg 6wt.%Al 0.5wt.%Mn.

The microstructures of the thixomolded AZ91 and AM60 sections comprised islands of primary α-Mg embedded in a matrix of α–Mg plus $(\alpha - Mg + Mg_{17}Al_{12})$ eutectic, see Fig. 1a and b. The AZ31 test sections had a fine equiaxed α-Mg microstructure having a grain size <10 μm, see Fig. 1c.

The spot welding equipment used in the present study had a rotational speed capability up to 3000 RPM while a servomotor provided axial loads up to 12 kN. Plunge rates up to 25 mm/s were selectable during spot welding, with the penetration depth being attained with an accuracy of ±0.1 mm. During friction stir spot welding the tool penetration (displacement) was measured using a linear transducer with an accuracy of ±0.01 mm while the axial load and torque were measured using a JR3 six-axis load cell, which was coupled to a data acquisition system. The key parameters (axial force, torque, rotational speed, pin displacement, shoulder and pin temperature) were logged during all spot welding trials.

The friction stir spot welding tool was machined from H13 tool steel, heat-treated to a hardness of 46–48 HRc, which minimized tool wear during spot welding. The tool used in the present study had a shoulder diameter of 10 mm, a pin diameter of 4 mm, a pin length of 2.2 mm and a simple threaded geometry. The tool shoulder and pin temperatures were measured by holding the pin stationary and rotating the AZ91, AZ31 and AM60 test samples. About 0.25 mm diameter K-type thermocouples were

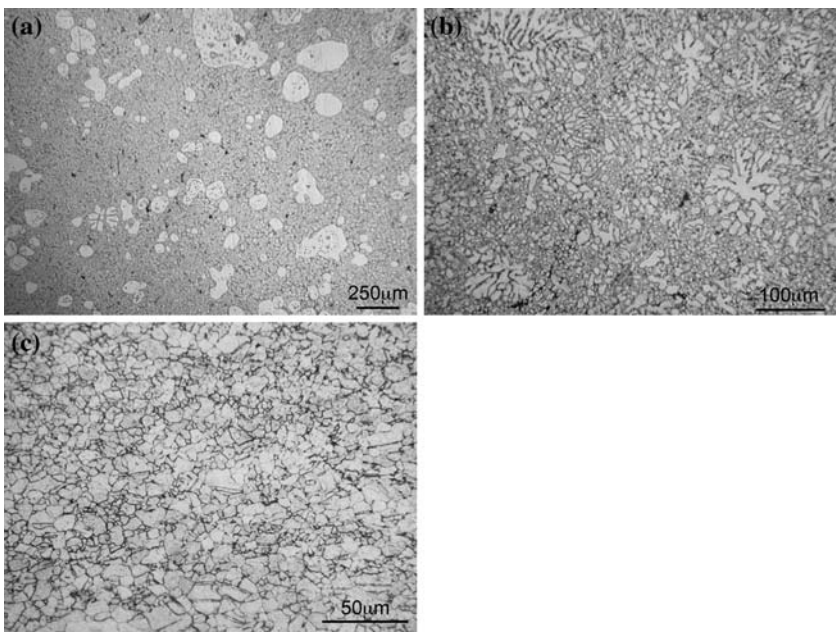

Fig. 1 Microstructures of (**a**) as-received thixomolded AZ91, (**b**) thixomolded AM60 and (**c**) wrought AZ31 test sections

inserted into 1.0 mm diameter holes in the tool assembly, in such a way that the tips of the thermocouples were directly in contact with plasticized material during spot welding. In each case the peak temperature was measured 0.2 mm from the tip of the pin while the shoulder temperature was measured at a location 1.5 mm from the shoulder periphery. It has been shown elsewhere that the temperature measurement set-up produces results, which are ±6.4 °C about the mean value during the dwell period in spot welding [12].

The thermal cycles in locations parallel to the tool axis during AZ91, AZ31 and AM60 spot welding were measured by locating 0.25 mm diameter thermocouples at distances of 2 mm (AZ91), 3 mm (AZ31) and 4 mm (AM60) from the pin periphery prior to spot welding. During testing the tips of the drilled holes were level with the bottom of keyhole. The exact locations of the thermocouples relative to the periphery of the rotating pin were determined following sectioning and metallographic examination.

It has already been shown that the LPI cracking tendency can be monitored by measuring the amount of stir zone material removed by the rotating pin when it is withdrawn at any selected dwell time [8]. The cracking tendency is the amount of the stir zone material created during spot welding, which is removed when the rotating tool is withdrawn at any dwell time setting. In this study the amount of material removed by the rotating tool when it is withdrawn at different dwell time settings was determined by weighing the AZ91, AZ31 and AM60 test sections before and after spot welding using a Mittler Toledo International Inc. AE160 weighing machine having an accuracy of ±0.1 mg.

Cracking during the dwell period in AZ91, AZ31 and AM60 spot welding was also investigated via high-speed imaging of material expelled at the periphery of the tool shoulder. The high-speed imaging set-up during friction stir spot welding is shown in Fig. 2. High-speed imaging was carried out using a Redlake Imaging Corporation Motion Scope PCI-1000-S camera using a frame speed of 500 fps.

The width of the stir zone formed adjacent to the periphery of the rotating pin at selected dwell times during AZ91, AZ31 and AM60 spot welding was measured halfway between the tip of the rotating pin and the tool shoulder.

The surfaces of the keyhole regions produced during AZ91, AZ31 and AM60 spot welding were examined using a combination of scanning electron microscope (SEM) and energy dispersive X-ray spectroscopy (EDX) analysis. All metallographic sections were etched in either 5–10 vol.% nital solution and/or acetic-picral solution comprising 10 mL acetic acid, 4.2 g picric acid, 10 mL H_2O and 70 mL of 95% ethanol.

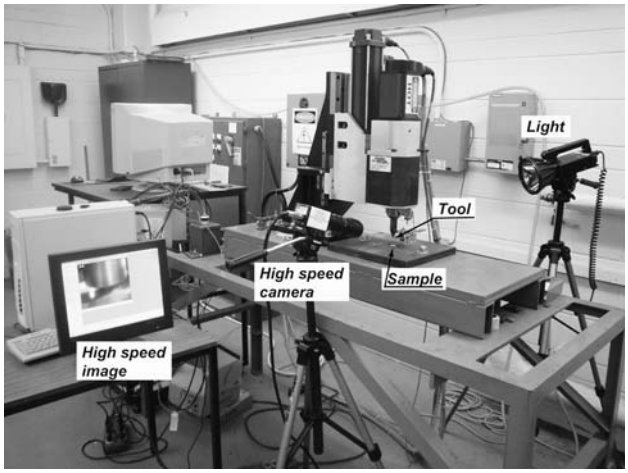

Fig. 2 High-speed imaging set-up when examining material expelled from the periphery of the tool shoulder during the dwell period in spot welding

Results

Figure 3a–c show the peak temperatures attained in the stir zones of AZ91, AZ31 and AM60 friction stir spot welds. The highest temperature is produced in the stir zone during AZ31 spot welding, e.g. the thermocouples located within the tool shoulder and 0.2 mm from the tip of the rotating pin reach 550 °C and 514 °C. Lower peak temperatures are produced in the stir zones of thixomolded AZ91 and AM60 spot welds. Also, the temperature varies during the dwell period in AZ91 spot welding, from 453 °C at the beginning of the dwell period to 438 °C at the end of the 4 s long dwell period; see Fig. 3a.

Figure 4a and b show the temperature cycles produced when thermocouples are positioned in drilled holes parallel to the periphery of the rotating pin. The temperature reaches 410 °C in the TMAZ region of AZ31 spot welds at a distance of 3.4 mm from the periphery of the rotating pin. A similar temperature is attained at the location 2.1 mm from the keyhole periphery in AZ91 spot welds. It is worth noting that it is extremely difficult to determine the temperature cycle in the TMAZ region at particular locations relative to the periphery of the rotating pin with consistency since thermocouples, which are contained within drilled holes are displaced outwards and downwards when the stir zone width increases during the dwell period in spot welding [6].

Figure 5 shows the microstructural features of the stir zones produced in AZ31 and AM60 spot welds. In AZ31 and AM60 spot welds the entire stir zone comprises fine equiaxed α-Mg grains having diameters <10 μm m, see Fig. 5a and b. However, Fig. 6a shows evidence of liquid penetration and cracking in the stir zone of an AZ91 spot weld close to its extremity while Fig. 6b shows a $Mg_{17}Al_{12}$ film at an α-Mg grain boundary region.

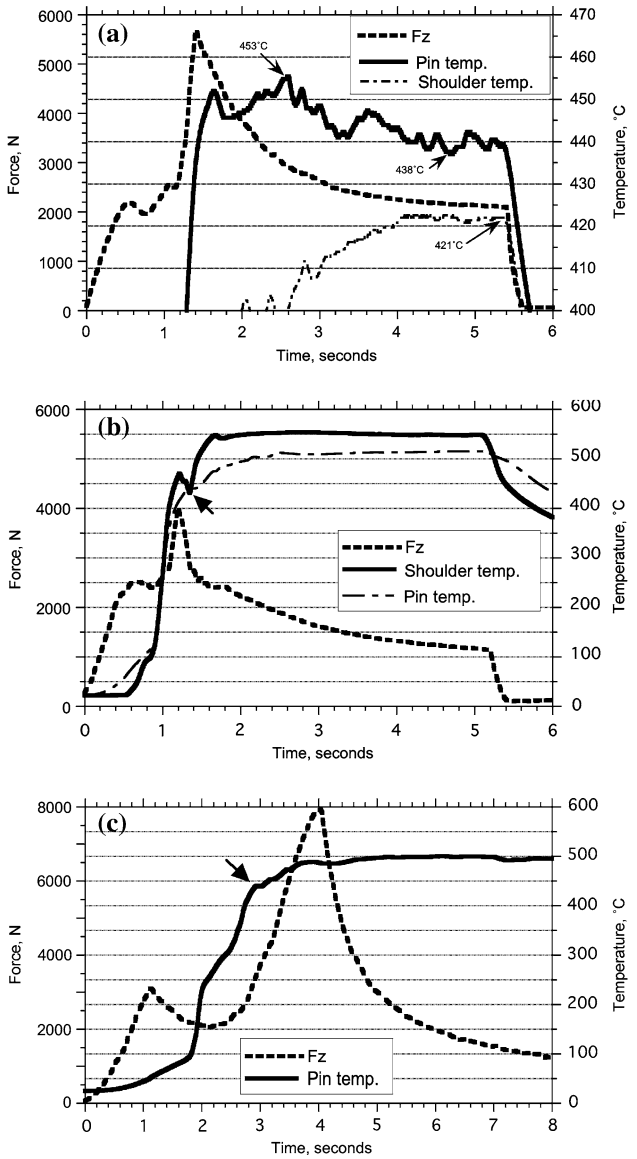

Fig. 3 Temperature and axial force output during spot welding of (**a**) thixomolded AZ91, (**b**) wrought AZ31 and (**c**) thixomolded AM60. The tool rotational speed was 3000 RPM for AZ91 and AZ31, 2500RPM for AM60. The plunge rate was 2.5 mm/s for AZ91 and AZ31, 1 mm/s for AM60

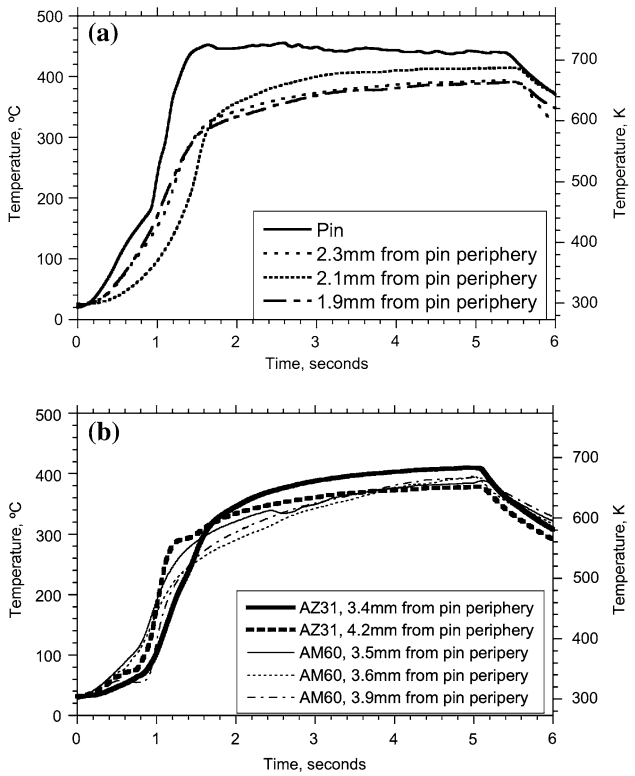

Fig. 4 (**a**). Temperature output at distances of 1.9 mm, 2.1 mm and 2.3 mm from the periphery of the rotating pin during AZ91 spot welding. In spot welds produced using a tool rotational speed of 3000 RPM, a plunge rate of 2.5 mm/s and a dwell time of 4 s. (**b**) Temperature cycles at distances of 3.4 mm and 4.2 mm from the periphery of the rotating pin during AZ31 spot welding and at distances of 3.5 mm, 3.6 and 3.9 mm from the periphery of the rotating pin during AM60 spot welding. In spot welds produced using a tool rotational speed of 3000 RPM, a plunge rate of 2.5 mm/s and a dwell time of 4 s

Figure 7a and b show profile of the cracked regions following tool removal at the end of the dwell period in AZ91 and AM60 spot welding. It is apparent that almost the entire stir zone is removed when the tool is withdrawn during AZ91 spot welding. In direct contrast, the stir zone formed during AM60 spot welding is clearly discernible

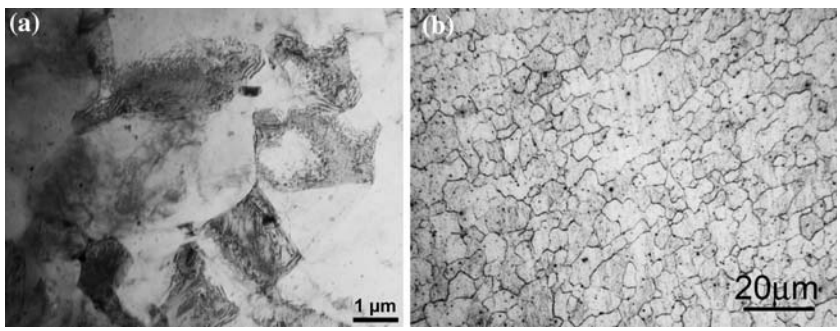

Fig. 5 (**a**) TEM micrograph showing fine-grained a-Mg in the stir zone of an AZ31 spot weld; (**b**) Fine-grained a-Mg microstructure in the stir zone of an AM60 spot weld. In each case, the plunge rate was 2.5 mm/s, the tool rotational speed was 3000 RPM and the dwell time was 4 s

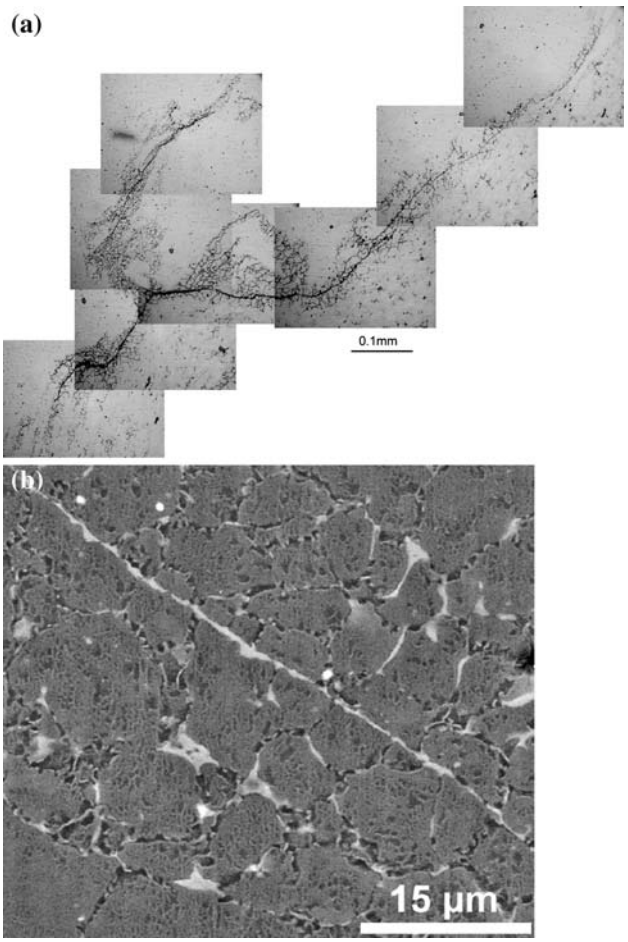

Fig. 6 (**a**) Penetration and cracking at grain boundary regions in the stir zone in the location close to its extremity; (**b**) $Mg_{17}Al_{12}$ film outlining a grain boundary in the stir zone in the location close to its extremity. In AZ91 spot welds made using a tool rotational speed 3000 RPM and a dwell time of 4 s and plunge rates of (**a**) 25 mm/s (**b**) 2.5 mm/s

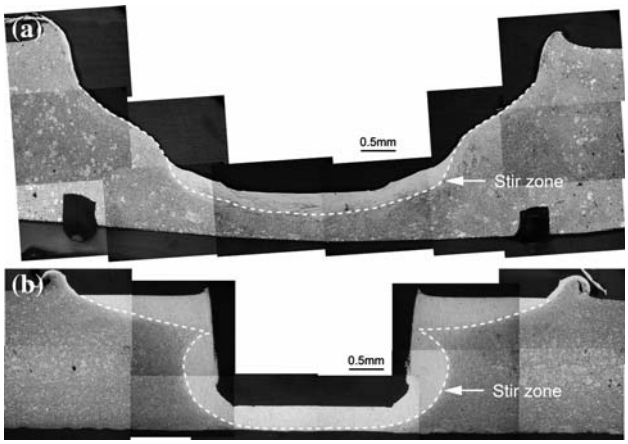

Fig. 7 (**a**) Removal of almost the entire stir zone when the rotating tool is withdrawn during AZ91 spot welding. In spot welds made using a tool rotational speed of 3000 RPM, a plunge rate of 2.5 mm/s and a dwell time of 4 s. (**b**) The profile of an AM60 spot weld following removal the rotating tool at the end of the spot welding operation. In spot welds made using a tool rotational speed of 3000 RPM, a plunge rate of 2.5 mm/s and a dwell time of 4 s

adjacent to the keyhole periphery following retraction of the rotating tool, see Fig. 7b. Similar output to that in AM60 spot welding is found when AZ31 spot welds are examined.

Figure 8a and b shows regions comprising $Mg_{17}Al_{12}$ and $(\alpha - Mg + Mg_{17}Al_{12})$ eutectic on the surfaces of keyholes produced during AZ91 spot welding using a plunge rate of 2.5 mm/s. The chemical composition of location A in Fig. 8a is similar to that found when examining the eutectic material produced during dissimilar Al 6111/AZ91 friction stir spot welding [13]. Also, locations B and C in Fig. 8b have chemical compositions corresponding with $Mg_{17}Al_{12}$.

The amount of stir zone material removed by the rotating tool when it is withdrawn varies with the dwell time applied during AZ91 spot welding; see Fig. 9. The amount of material removed when the tool is withdrawn markedly increases early in the dwell period, reaches a maximum value when the dwell time is around 2 s and then decreases when the dwell time is extended to 4 s. In contrast, the amount of material removed by the rotating tool when it is withdrawn is unchanged during the dwell period in AZ31 and AM60 friction stir spot welding.

Figure 10 shows the high-speed imaging output produced during AZ91 spot welding using different dwell times. Early in the dwell period material expelled from the shoulder periphery is displaced circumferentially and moves with the rotating shoulder as it rotates. Circumferential displacement of expelled material is apparent for dwell times from 0.1 s to 2 s and then ceases when the dwell time increases to 4 s during AZ91 spot welding. This experimental output is consistent with crack formation early in the dwell period, with the cracking tendency being highest when a dwell time of 2 s is applied. However, quite different test results are produced during AZ31 and AM60 spot welding. Circumferential movement of expelled material from the periphery of the tool shoulder is only apparent very early in the dwell period (when dwell times of 0.05 and 0.1 s are used). However, there is no evidence of circumferential displacement of expelled material from the periphery of the rotating tool when dwell times >0.1 s are applied during AZ31 and AM06 spot welding.

Figure 11a–c show evidence of eutectic melting and cracking in the TMAZ region immediately adjacent to the stir zone extremity in AZ91, AM60 and AZ31 spot welds produced using dwell times of 0.05 and 0.1 s. In this connection, discontinuities are apparent on the temperature output produced during AM60 and AZ31 spot welding; see

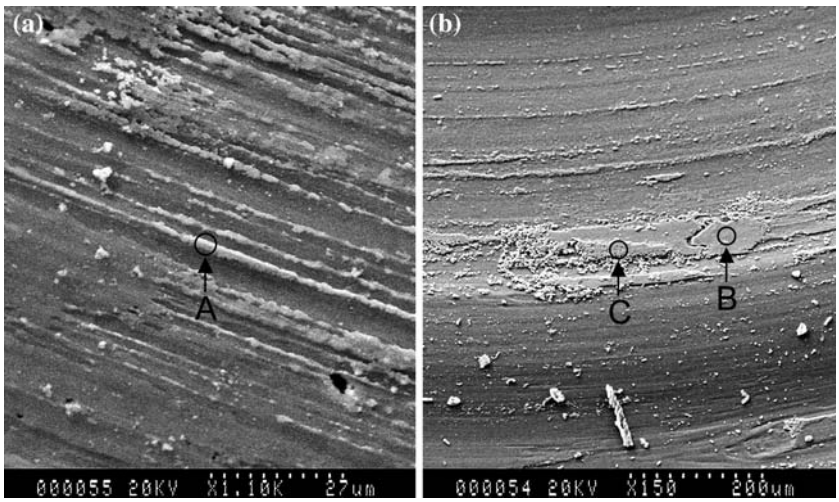

Fig. 8 SEM examination of the keyhole surfaces in an AZ91 spot weld. (**a**) EDX analysis at location A indicated the chemical composition: 73.9wt% Mg, 26.1wt% Al. (**b**) EDX analyses at locations B and C indicated chemical compositions: 50.8wt% Mg, 45.8wt% Al and 51.4 wt% Mg, 45.9 wt% Al. In each case, the plunge rate was 2.5 mm/s, tool rotational speed was 3000 RPM and a dwell time of 4 s

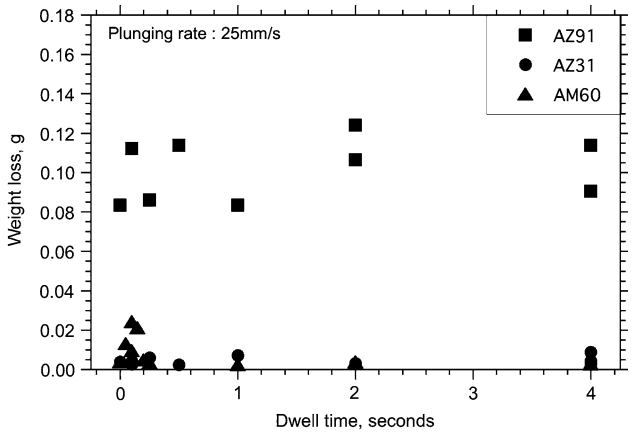

Fig. 9 Amount of stir zone material removed when the rotating tool is withdrawn for different dwell times during AZ91, AZ31 and AM60 spot welding. The plunge rate was 25 mm/s and the tool rotational speed was 3000 RPM

the locations highlighted by arrows in Fig. 3b and c. These discontinuities occur at temperatures, which are close to the $\alpha - Mg + Mg_{17}Al_{12}$ eutectic temperature (437 °C).

Detailed metallographic examination of AZ91, AZ31 and AM60 spot welds produced using dwell times > 0.1 s showed no evidence of cracking in the TMAZ regions.

Discussion

The change in the amount of material removed by the rotating tool when it is withdrawn (Fig. 9), high-speed imaging output confirming circumferential displacement of expelled material from the periphery of the tool shoulder during the dwell period (Fig. 10), confirmation of $Mg_{17}Al_{12}$ and $(\alpha - Mg + Mg_{17}Al_{12})$ eutectic regions on the keyhole surfaces (Fig. 8) and the removal of almost the entire stir zone when the rotating tool is withdrawn (Fig. 7a) support the contention that cracking occurs during the dwell period in AZ91 spot welding. Also, Fig. 11a indicates that cracking occurs in the TMAZ region very early in the dwell period and the cracking tendency is highest when a dwell time of 2 s is applied during AZ91 spot welding.

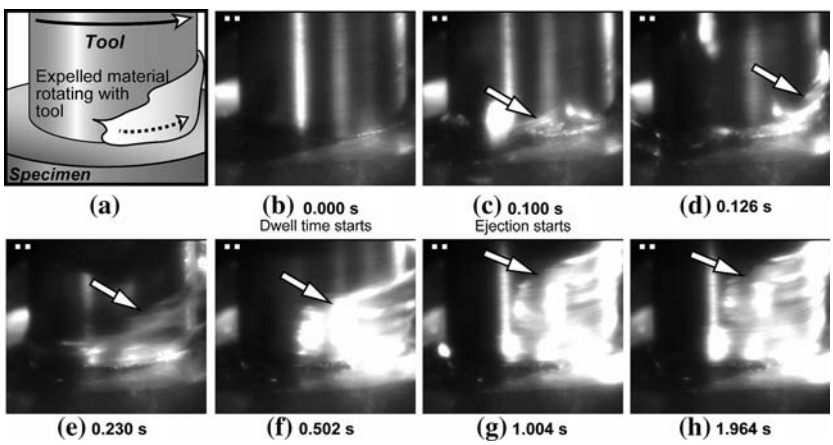

Fig. 10 High-speed imaging output showing circumferential displacement of expelled material at the periphery of the tool shoulder. In AZ91 spot welds made using a tool rotational speed of 3000 RPM and a plunge rate of 25 mm/s (after Ref. 8)

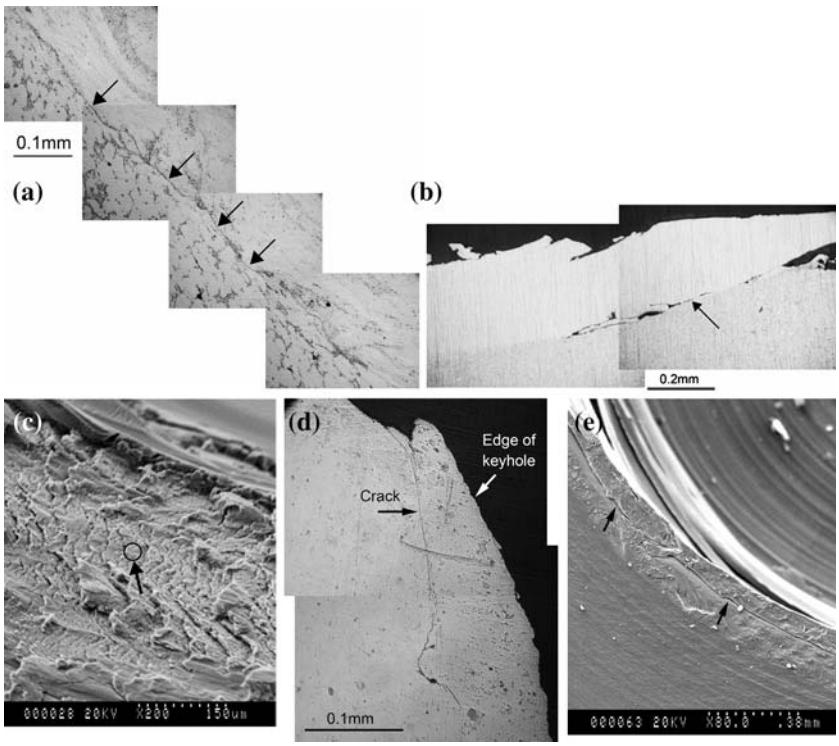

Fig. 11 Cracking in the TMAZ region of AZ91, AM60 and AZ31 friction stir spot welds made using dwell times of 0.05 s (AZ31) and 0.1 s (AZ91 and AM60). (**a**) Cracking in the TMAZ of an AZ91 spot weld, see arrows. (**b**) Cracking in the TMAZ of an AM60 spot weld, see arrows. (**c**) Cracking surface in the TMAZ of an AM60 spot weld; the chemical composition at the location indicated on the keyhole surface is 79.0 wt% Mg, 20.9 wt% Al. (**d**) Cracking in the TMAZ of an AZ31 spot weld, see arrows. (**e**) Cracking immediately adjacent to the keyhole periphery in the TMAZ of an AZ31 spot weld (see arrows)

In contrast, the amount of material removed by the rotating tool when it is withdrawn during AZ31 and AM60 spot welding is unchanged during the dwell period. However, in both cases high-speed imaging confirmed the circumferential displacement of expelled material from the shoulder periphery very early in the dwell period (when dwell times of 0.05 and 0.1 s are applied). Figure 11b and c also show evidence of cracking in the TMAZ regions in AZ31 and AM60 spot welds made using dwell times of 0.05 and 0.1 s. However, AZ31 and AM60 spot welds produced using dwell times > 0.1 s are crack-free.

With this in mind, it is proposed that cracking during AZ91, AZ31 and AM60 friction stir spot welding is determined by the following sequence of events:

a) Formation of melted eutectic films and cracking in the TMAZ region in the locality immediately adjacent to the stir zone extremity very early in the dwell period (when the dwell times of 0.05 and 0.1 s are applied); see Fig. 11.
b) Engulfment of melted eutectic films when the stir zone increases in width during the dwell period in spot welding, see Fig. 12. When melted eutectic films formed in the TMAZ region are engulfed this provides the conditions for penetration of α-Mg grain boundaries in the stir zone close to its extremity. Much of the research examining liquid metal embrittlement has highlighted the crack initiation stage rather than the crack propagation stage in failure since liquid film penetration at grain boundary regions is extremely rapid [14, 15]. Consequently, engulfment of melted eutectic films formed in the TMAZ region facilitates rapid penetration of α-Mg grain boundaries in the stir zone close to its extremity.
c) Crack propagation due to the torque applied by the tool as it rotates during the dwell period. Tool withdrawal per se does not promote cracking in the location closed

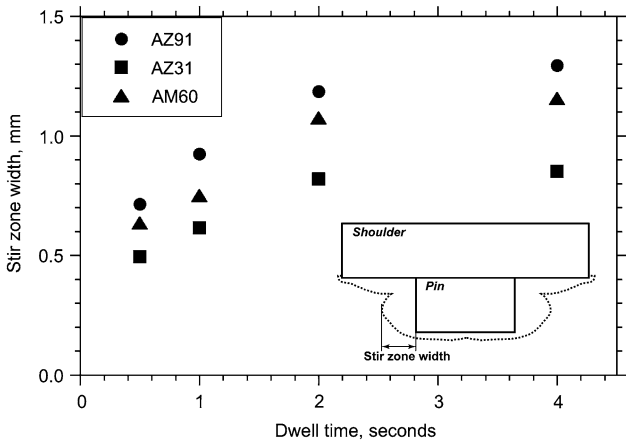

Fig. 12 Variation in stir zone width during the dwell period in AZ91, AZ31 and AM60 spot welding. In spot welds made using a plunge rate of 2.5 mm/s and a tool rotational speed of 3000 RPM

to the stir zone extremity. The axial movement upwards of the rotating tool when the spot welding operation is terminated merely separates sections, which are already cracked.

d) Diminished cracking tendency when the dwell time increases beyond 2 s during AZ91 spot welding. In AZ31 and AM60 spot welds cracking is only apparent very early in the dwell period (when dwell times of 0.05 and 0.1 s are applied).

Recent research has confirmed that the temperature cycle within the stir zone cannot be determined by locating thermocouples in drilled holes parallel to the periphery of the rotating pin prior to friction stir spot welding since the helical vertical rotational flow generated within the stir zone during the dwell period displaces thermocouples from their original locations [6]. However, Fig. 3a indicates that the temperature is very close to 437 °C at the end of the dwell period in AZ91 spot welding while Fig. 6a shows penetration of α-Mg grain boundaries. Since the temperature in the TMAZ region at a distance of 2.1 mm from the keyhole periphery is 410 °C (see Fig. 4a) it can be assumed that the temperature near the stir zone extremity is close to 437 °C, the $\alpha - Mg + Mg_{17}Al_{12}$ eutectic temperature. In this connection, it has been recently suggested that the set-up of a helical vertical rotational flow of material within the stir zone formed adjacent to the periphery of the rotating tool facilitates the establishment of a uniform temperature across the width of the stir zone formed adjacent to the periphery of the rotating pin [16].

It has been recently suggested that the decreased cracking tendency when the dwell period is extended during AZ91 spot welding is caused by the competing effects produced by dissolution of melted eutectic films and material incorporation [8]. When melted eutectic films form in the TMAZ region early in the dwell period and are engulfed as the stir zone grows in width during the dwell period, dissolution will occur at the following temperatures: 437 °C and 460 °C (in AZ91 spot welds), 500 °C (in AM60 spot welds) and 514 °C and 550 °C (in AZ31 spot welds).

The dissolution kinetics of plate-shaped melted eutectic films at any given temperature can be evaluated using Whelan [17] and Reiso's methodology [18], see the Appendix. The time required for dissolution of a plate-shaped liquid film is determined by the relation:

$$B = B_o - \frac{k}{\sqrt{\pi}}\sqrt{Dt}$$

where B is half the thickness of the liquid film, B_o is half the initial film thickness, $k$is the thermodynamic driving force for dissolution, D is the solute diffusion coefficient at any selected temperature.

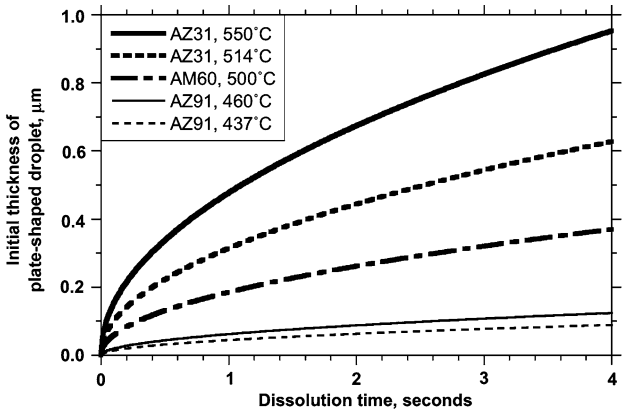

Fig. 13 Relation between the width of a plate-shaped film of melted eutectic and the dissolution time when temperatures of 437, 460, 500, 514 and 550 °C are assumed

Figure 13 shows the relation between the thickness of plate-shaped melted eutectic films and the dissolution time at 437, 460, 500, 514 and 550 °C. The dissolution rate is much slower during the dwell period in AZ91 spot welding, e.g. a 125 nm thick film of melted eutectic will dissolve in about 4 s. However, it is apparent from Fig. 6b that 0.5–1.5 µm thick $Mg_{17}Al_{12}$ films are present at α-Mg grain boundary regions in the stir zone close to its extremity. As a result, it would be expected that AZ91 friction stir spot welds made using a dwell time of 4 s would exhibit LPI cracking within the stir zone.

However, the dissolution rate of eutectic films is much more rapid during AM60 and AZ31 spot welding since much higher stir zone temperatures are produced, see Fig. 3b and c. Following their engulfment by the growing stir zone melted eutectic films will dissolve very rapidly and although TMAZ cracking is apparent early in the dwell period (in spot welds made using dwell times of 0.05 and 0.1 s) crack-free spot welds are produced when a dwell time of 4 s is applied.

The mechanism of cracking during the dwell period in spot welding is quite different from that when liquation cracking occurs in the HAZ region of fusion welds. During fusion welding, liquation cracking results from the combined effects of high HAZ temperatures, which exceed the melting point of local regions of pre-existing chemical segregation in the as-received base material and tensile straining when the welded joint cool to room temperature [19]. However, the proposed LPI cracking mechanism is dynamic in character since failure in the stir zone is determined by a string of consecutive events involving eutectic melting in the TMAZ region, engulfment of melted films by the growing stir zone, penetration of α-Mg grain boundaries and crack propagation resulting from tool rotation during the actual welding operation. Dissolution of

melted eutectic films and material incorporation continue during the dwell period spot welding with the stir zone temperature having a determining influence since the dissolution rate of melted eutectic films markedly increases at temperatures >437 °C. In AZ91 spot welds dissolution does not occur fast enough to prevent LPI cracking. However, in AM60 and AZ31 spot welds higher stir zone temperatures mean that the dissolution rate is much faster and crack-free welds are produced when a dwell time of 4 s is applied.

Conclusions

Liquid penetration induced cracking in AZ91, AZ31 and AM60 friction stir spot welds has been investigated. It has been shown that:

1. Cracking occurs early in the dwell period in AZ91 spot welding and almost the entire stir zone is removed when the rotating tool is withdrawn. In contrast, cracking in AZ31 and AM60 spot welds is only apparent very early in the dwell period, when dwell times of 0.05 and 0.1 s are applied. When the dwell times >0.1 s are used, crack-free AZ31 and AM60 spot welds are produced.
2. LPI cracking in AZ91 spot welds involves the following sequence of events: melted eutectic film formation in the TMAZ region immediately adjacent to the stir zone extremity, engulfment of melted eutectic films as the stir zone grows in width during the dwell period, penetration of α-Mg grain boundaries in the stir zone close to its extremity and crack propagation due to the torque applied by the rotating tool.
3. The temperature produced in the stir zone during Mg-alloy friction stir spot welding has a determining influence on LPI cracking. Since the stir zone temperatures in AZ31 and AM60 spot welds are much higher than the $\alpha - Mg + Mg_{17}Al_{12}$ eutectic temperature (437 °C) melted eutectic films dissolve rapidly following their engulfment by the growing stir zone and crack-free joints are produced when a dwell time of 4 s is applied. However, since the temperature during the dwell period in AZ91 spot welding is close to 437 °C, melted eutectic films are not completely dissolved and friction stir spot welds produced using a dwell time of 4 s exhibit LPI cracking.

Acknowledgements The authors wish to acknowledge financial support from the Natural Sciences and Engineering Research Council of Canada during this project.

Appendix

Dissolution of a Melted Eutectic Films during AZ91, AM60 and AZ31 Spot Welding

Figure A.1 shows part of the binary Mg–Al equilibrium phase diagram:

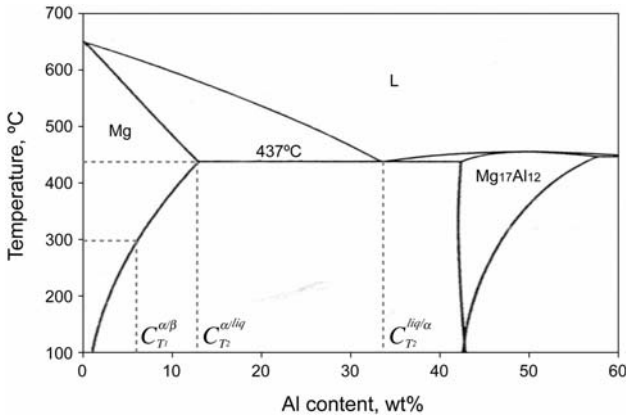

Fig. A.1 Binary equilibrium phase diagram for Mg–Al

The driving force for diffusion and dissolution of liquid droplets is determined by the relation:

$$k = 2\left[\frac{C_{T_2}^{\alpha/liq} - C_{T_1}^{\alpha/\beta}}{C_{T_2}^{liq/\alpha} - C_{T_2}^{\alpha/liq}}\right]$$

For AZ91; k = 0.4, $C_{T_1}^{\alpha/\beta} = 9\%$, $C_{T_2}^{\alpha/liq} = 13\%$, $C_{T_2}^{liq/\alpha} = 33\%$, $T_2 = 710\,\mathrm{K}$

For AM60; k = 0.7, $C_{T_1}^{\alpha/\beta} = 6\%$, $C_{T_2}^{\alpha/liq} = 13\%$, $C_{T_2}^{liq/\alpha} = 33\%$, $T_2 = 710\,\mathrm{K}$

For AZ31; k = 1.0, $C_{T_1}^{\alpha/\beta} = 3\%$, $C_{T_2}^{\alpha/liq} = 13\%$, $C_{T_2}^{liq/\alpha} = 33\%$, $T_2 = 710\,\mathrm{K}$

The diffusion coefficient depends on the relation:

$$D = D_o \exp\left[-\frac{Q}{RT}\right]$$

where$R = 8.314 \times 10^{-3}$ kJ/(mol · K) and the diffusion rate of Al in Mg is [20]:

$$D_o = 1.53 \times 10^7\ \mu\mathrm{m}^2/\mathrm{s}, \quad Q = 125\mathrm{kJ/mol}$$

For AZ91;

$$D_{\mathrm{Al\,in\,Mg\,at\,710\,K}} = 9.73 \times 10^{-3}\ \mu\mathrm{m}^2/\mathrm{s} \quad \text{at } 710\,\mathrm{K}(437\,^\circ\mathrm{C})$$

$$D_{\text{Al in Mg at 733 K}} = 1.89 \times 10^{-2}\,\mu\text{m}^2/\text{s} \quad \text{at } 733\,\text{K}(460\,^\circ\text{C})$$

For AM60;

$$D_{\text{Al in Mg at 773 K}} = 5.47 \times 10^{-2}\,\mu\text{m}^2/\text{s} \quad \text{at } 773\,\text{K}(500\,^\circ\text{C})$$

For AZ31;

$$D_{\text{Al in Mg at 787 K}} = 7.73 \times 10^{-2}\,\mu\text{m}^2/\text{s} \quad \text{at } 787\,\text{K}(514\,^\circ\text{C})$$

$$D_{\text{Al in Mg at 823 K}} = 1.78 \times 10^{-1}\,\mu\text{m}^2/\text{s at } 823\,\text{K}(550\,^\circ\text{C})$$

The relation between the half-thickness of a plate-shaped liquid droplet and the time available for dissolution at 710, 733, 773, 787 and 823 K is determined by the relation:

$$B_0 = \frac{k}{\sqrt{\pi}}\sqrt{D_{\text{Al in Mg at (710,733,773,787,823)K}} \cdot t}$$

It is worth noting that this equation is a first order approximation and is derived by assuming no overlapping of the concentration fields from neighboring films.

References

1. Gerlich A, Su P, North TH, In: Neelameggham NR, Kaplan HI, Powell BR (TMS, 2005) Magnesium Technology 2005. pp 383–388
2. Su P, Gerlich A, North TH, SAE Technical Series, 2005-01-1255
3. Aritoshi M, Tomita T, Ikeuchi K, Takahashi M, Tani K, M. Ueda and Sakurai T, Preprints of the National Meeting of Jpn Weld Soc (2006.9) 123 (in Japanese)
4. Ikegami H, Tsumura T, Ueda M, Nakata K, Preprints of the National Meeting of Jpn Weld Soc (2006.9) 141 (in Japanese)
5. Yamamoto M, Su P, Gerlich A, North TH, Shinozaki K (2007) J Jpn Weld Soc 25(1):208 (in Japanese)
6. Yamamoto M, Su P, A. Gerlich and North TH, SAE Technical Series, (2007), #2007-01-1700
7. Yamamoto M, Gerlich A, North TH, Shinozaki K (2007) accepted in Proc IWJC-Korea Int Weld./Joining Conf, Seoul, Korea, May 2007
8. Yamamoto M, Gerlich A, North TH, Shinozaki K (2007) Sci Tech Weld Joining 12(3):208
9. SU P, Gerlich A, Yamamoto M, North TH (2006) In: Pekguleryuz MO, Mackenzie LWF (eds) Proc Int Symp on 'Magnesium technology in the global age', Montreal, Canada, October 2006, CIM, pp 479–492
10. Japan Magnesium Association (2000) In: Handbook of advanced magnesium technology. Kallos Publishing, Japan, p 90
11. Bassani P, Gariboldi E, Tuissi A (2005) J Thermal Anal Calorimet 80:739
12. Gerlich A, Cingara GA, North TH (2006) Metall Trans 37A:2773
13. Gerlich A, Su P, North TH (2005) Sci Tech Weld Joining 10(6):647
14. Fernandes PJL, Jones DRH (1997) Int Mat Rev 42(6):251
15. Ludwig W, Pereiro-lopez E, Bellet D (2005) Acta Mater 53:151
16. Su P, Gerlich A, North TH, Bendzsak GJ (2007) Metall Trans 38A:584
17. Whelan MJ (1969) Met Sci J 3:95
18. Reiso O, Overlie H-G, Ryum N (1990) Metall Trans 21A:1689
19. Lathabai S, Barton KJ, Harris D, Lloyd PG, Viano DM, Mclean A (2003) In: Magnesium Technology 2003. Kaplan HI (TMS, 2003), pp 157–162
20. Japan Magnesium Association (2000) In: Handbook of advanced magnesium technology. Kallos Publishing, Japan, p 132